CWP-423
May 2002

Seeing heterogeneities in rocks: Preliminary results from a noncontacting ultrasonic experiment

Alison Malcolm & John Scales

This paper appeared in the May 2002 CWP Project Review, CWP-425.

Center for Wave Phenomena
Colorado School of Mines
Golden, Colorado 80401
303/273-3557

Seeing heterogeneities in rocks: Preliminary results from a noncontacting ultrasonic experiment

Alison Malcolm and John Scales
Center for Wave Phenomena, Colorado School of Mines

ABSTRACT

Using lasers to excite and detect ultrasonic waves, we are able to make rapid and repeatable measurements of wave propagation in rocks, which are heterogeneous, granular media. We study two cylindrical granite samples with similar elastic moduli and attenuation coefficients, but different average grain sizes. In both we see clear evidence of fracture-induced anisotropy in the first-arriving compressional waves, with an 11% difference between the fast and slow directions. We have recorded very long timeseries to enable us to study other effects such as multiple scattering. In the medium-grained granite (ratio of dominant wavelength to average grain size about 10) we see coherent events throughout the dataset; for example, surface waves that have made up to six circumnaviations of the sample. However, in the coarse-grained sample (wavelength to grain size ratio about 2) even though the entire data set is above the ambient noise level, the data show rapid de-coherence due to scattering from the granular microstructure.

These rapid, noncontacting techniques open up many new possible rock properties measurements that would be difficult or impossible with contacting transducers, such as three dimensional microtomography and surface scanning measurements. The laser source provides a clean input signal that can be optically shaped and is not distorted by the mechanical response of a transducer. The laser detector gives an absolute measure of particle velocity, and the vibration isolation system we use allows us to make high-fidelity recordings of amplitude and phase for extremely long waveforms. We hope to be able to exploit multiply scattered waves to make inferences about the microstructure of rocks, develop new methods of imaging seismic data with diffuse waves, and to verify new effective medium (upscaling) theories of wave propagation in random media.

Key words: laser ultrasonics, multiple scattering, surface waves, anisotropy

Introduction

Heterogeneous media appear homogeneous when probed with waves whose wavelength is large compared to the scale of heterogeneity. As the wavelength decreases relative to the heterogeneity, scattering from the microstructure becomes important. In many types of rocks rocks, this microstructure is random. If it is possible to make an ensemble of measurements that differ only in the way they sample the random microstructure, then in principle these differences can be exploited to make inferences about the average scattering properties of the microstructure. This idea has been exploited recently by De Rosny and Roux (2001) and Scales and Van Wijk (2001) to infer the mean free scattering path in disordered media using multiply-scattered ultrasonic waves. In this paper we report on preliminary measurements of ultrasonic multiple scattering in two granite samples using lasers as sources and detectors of elastic waves in a non-contacting experiment.

De Rosny and Roux (2001) show how multiply scattered acoustic waves can be used to count fish in a

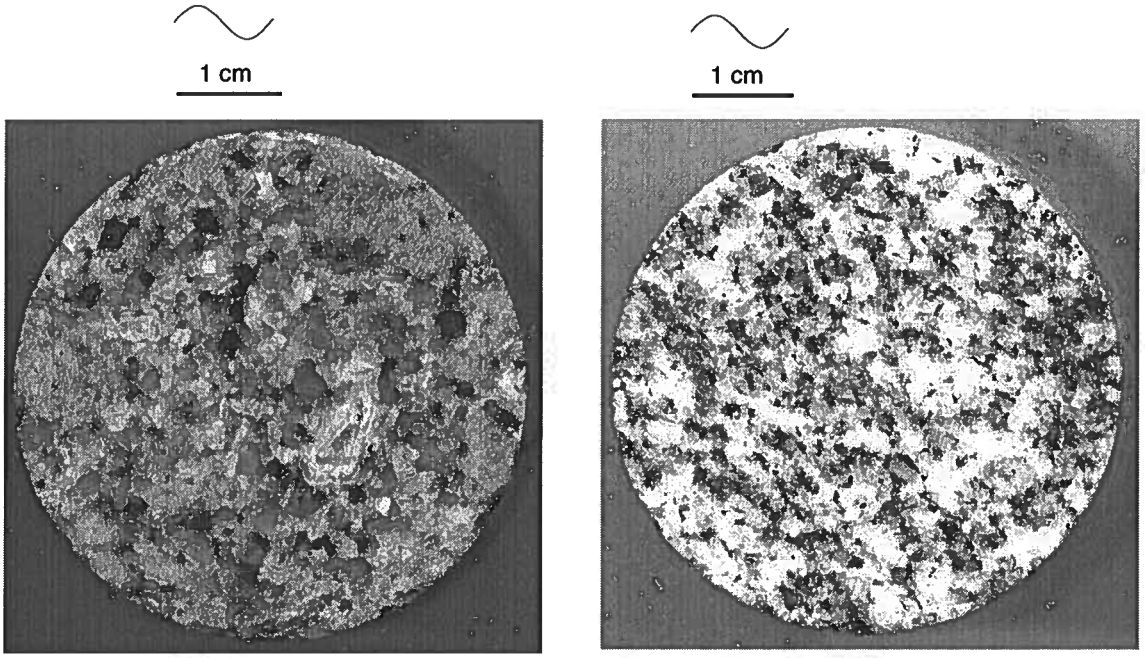

Figure 1. Scanned surfaces of the rock samples used in this experiment, the Llano is shown on the left, the Elberton on the right. The average grain sizes are approximately 1 mm for the Elberton and 4 mm for the Llano. The wavelengths shown are approximate and are based on a 500 kHz peak frequency and 4.5 mm/μs velocity.

tank.Their premise is that the scattering off of the walls of the tank is constant, no matter what the position of the fish, while the scattering due to the fish changes because of their movement. In this way they are able to make an ensemble of measurements which differ only in the location of the scatterers by simply waiting for the fish to move between measurements. We attempt to use similar ideas to characterize the scattering properties of rock samples. We have chosen granite samples to begin with since granites vary in grain size while other properties, such as the velocity, composition and attenuation are similar.

We use two samples, with different grain sizes (see figure 1) and similar velocities and Q values, to demonstrate the differences in the data in the presence and absence of grain scattering. The initial step in our experiment is to collect an ensemble of measurements which vary only in how they have sampled the randomness of the medium. Perhaps the simplest way to collect such an ensemble is to exploit the geometrical symmetry of the sample, by taking data as a function of the angle ϕ (defined in figure 2) in a cylindrical sample for example, thus collecting data in which the signature of the sample's shape is independent of the realization. There are several other ways in which one could collect an ensemble of measurements, including: collecting data sets with the source and receiver locations fixed for an ensemble of frequencies, creating different realizations of the medium by mixing or recreating the material and using different samples of the same medium.

The immediate goal of this work is to be able to extract information from acoustic data about the heterogeneity of rock samples. From the data we have collected thus far we are able to see changes in the waveform between samples with different grain sizes, indicating that the heterogeneity is affecting the waveform in a way that our measurements are sensitive to. We hope to extract more quantitative information about these differences both from the data we have already obtained and from future experiments.

Experiment

The experimental set up is shown in figure 2. The source is a Spectron pulsed Nd:YAG laser which emits 5 ns pulses of 1.064 μm near IR photons with approximately 100 mJ per pulse. Using the collimated but unfocused beam (7 mm diameter), this power level is within the thermoelastic regime for the rock samples used in this experiment. The thermoelastic expansion of the rock surface generates the elastic waves. General properties of lasers and their applications to ultrasonics are discussed in Scruby and Drain (1990).

To detect the waveforms we used a laser-Doppler vibrometer (Polytec sensor head and vibrometer controller with a high-frequency decoder). The vibrome-

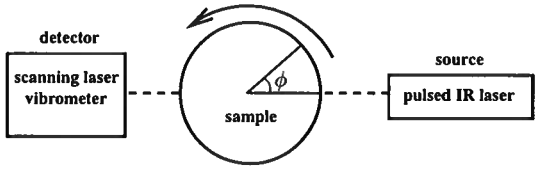

Figure 2. A cylindrical sample was placed between the laser source and detector. Here the source and detector are colinear, but any orientation is possible. The cylindrical sample is placed in a rotational stage and the angle phi is incremented from 0 to 360 degrees. The vibrometer measures absolute particle velocity along the detector beam.

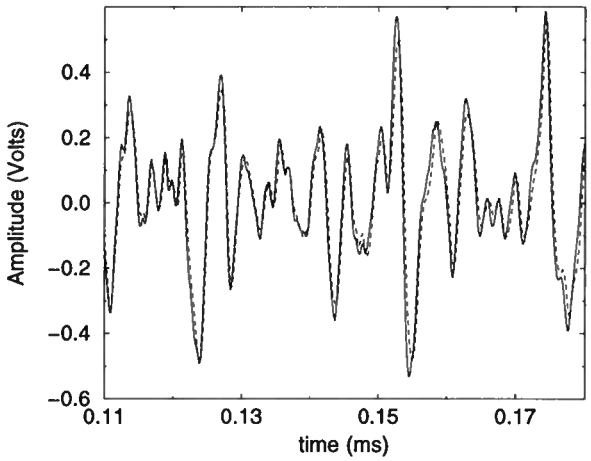

Figure 3. Two measurements taken at the beginning of the experiment (solid line) and the end of the experiment (dashed line) at the same location on the Elberton sample. The noncontacting nature of the experiment, along with the low noise level, allows repeatable data to be taken quickly and easily.

ter uses a 1 mW visible He-Ne laser in a heterodyne-interferometer arrangement to measure absolute particle velocity in the direction of the beam. The signal was amplified with a low-noise preamplifier (SR 560 with 12 db/octave 3 kHz high-pass filter) and digitized at 14-bit resolution using a Gage digital oscilloscope card attached to a PC.

Since we hope to have the coherent signal, such as the direct arrivals and surface waves, be consistent at each data point (i.e. each angle ϕ), it is important for the data to be repeatable. To help reduce the noise in our data, both lasers and the sample were mounted on an optical bench with vibration isolation legs. With this reduced noise level and the non-contacting nature of laser ultrasonics, we have been able to collect extremely repeatable data, as can be seen in figure 3.

For this experiment, the ensemble of measurements

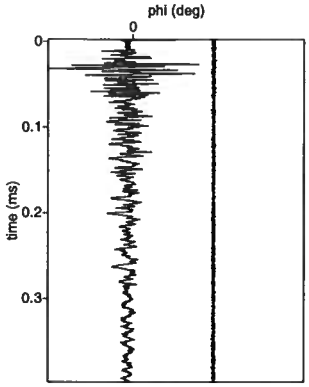

Figure 4. The trace on the left is the 0° Llano data, and the trace on the right is a noise trace recorded with the same setup but without a source. We can see that even at the end of our recording window our data have much larger amplitude than the noise. The two waveforms are plotted on the same scale.

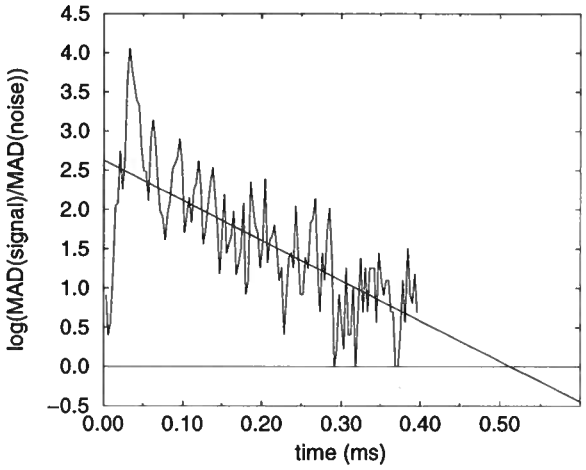

Figure 5. This plot shows the median average deviation, the signal has relaxed to the ambient noise level when it crosses the x-axis which in this case is outside the recording window. The slope of the line fit to the data gives a measure of Q. Computing Q from this slope gives Q=28, which is in agreement with the modal Q.

consists of 35 different waveforms, each taken at a different angle around the cylindrical samples in 10° increments. The sample was positioned using a manual rotation stage mounted on the vibration isolation table. The source laser is then turned on and 500 measurements are recorded and averaged as the final data. With this level of averaging, the noise level is much lower than

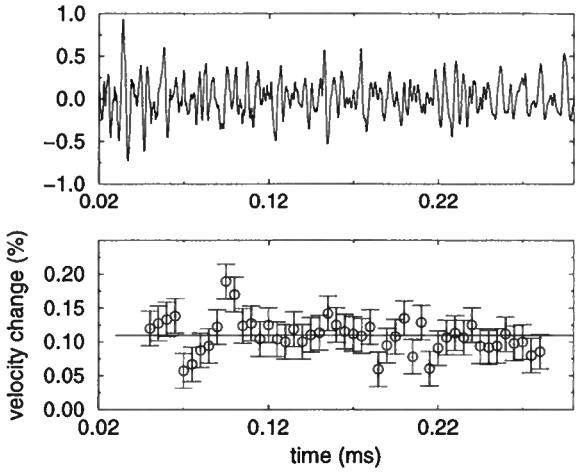

Figure 6. The data recorded at 0 and 360 degrees (i.e., after a complete rotation) should be the same. Plotted at this scale they are identical. However late in the coda there is a systematic dephasing due to the small temperature increase during the measurement. We use the technique of coda wave interferometry to infer a velocity change of 0.11%, which is the mean of the points plotted in the lower figure.

the signal level, even at the end of our record time, as is shown in figures 4 and 5.

Since we are using an infrared laser to excite waves in our sample, we expect the sample to heat up during the experiment. The wave velocity in granite changes with temperature so this could create errors in our experiment. We used the method of coda wave interferometry (Snieder *et al.*, 2002) to quantify the change in our sample's velocity as a function of temperature. To do this we recorded two traces, one at the beginning of our experiment and one at the end, at the same position on the sample. We then computed the average time lag between the two realizations to determine the velocity change due to the heating of the sample. This change was found to be approximately $0.1 \pm 0.025\%$, which is small in this experiment. The computed velocity change as a function of time window is shown in figure 6.

The samples and their characteristics

This experiment was performed on two samples with similar average velocities but significant differences in grain size (see figure 1). Because of this difference in grain size, we expect the two samples to have different scattering properties.

The Elberton sample is a medium-grained felsic granite. Because the grain size in this sample is much smaller than a wavelength, we do not expect to see strong effects of scattering. We know, due to geometrical spreading, that most of the energy at late times will come from the surface waves.

The Llano sample is a coarser grained pink granite. The grain size is approximately half of a wavelength, which is roughly four times larger than that of the Elberton granite. We thus expect some energy to be scattered from the grain boundaries and cracks in this sample. Both samples are shown in figure 1.

Attenuation measurements were made on both samples, and are shown in figure 7. These measurements were made with the method of resonance (Le Rousseau *et al.*, 2002). From these data we see that the two samples should have approximately the same attenuation properties. The Llano has a lower Q value but the difference is within the errors in the measurements assuming that the measurements made on the Llano sample have similar errors to those made on the Elberton.

For the Llano data, a noise trace was recorded and is shown in figure 4, from which we can compute the time for the signal to decay to the ambient noise level, giving another measure of Q. In figure 5 we see the log (base 10) of the median average deviation of the signal normalized by the noise. Assuming that the attenuation of the signal is of the form $A_0 e^{-\frac{\omega t}{2Q}}$ the slope of this curve gives a measure of Q. Using a frequency of 45 kHz, chosen to be compatible with the frequency range in figure 7, we compute $Q = 28$, which is lower than the values of Q shown in figure 7, although possibly still within the measurement errors. The difference may be due to losses into the sample holder.

Initial Experimental Results

Data, plotted as a function of the rotation angle ϕ, are shown in figures 9 - 12. All data sets use the same plot scaling, i.e., each plot has been scaled relative to the maximum values in the particular data set and this scaling is computed in the same way for all plots. There are several things that are apparent in the data. The first is that the two data sets have very different coherence levels, especially at late times. In the Elberton data we can see six different coherent surface arrivals even in the raw data (figure 9), while the Llano data quickly becomes incoherent. Since the attenuation properties of the two samples are similar, this indicates that the coherence is being reduced in the Llano sample by a mechanism not present in the Elberton sample. This is strong evidence of grain scattering. This is visible in the Llano granite and not in the Elberton because of its much larger grain size. In figure 10, agc gain has been applied to both data sets, with parameters chosen separately for each data set. On the Elberton data, the gain has enhanced the surface waves. These events are now also visible in the Llano data set, although they are still not as strong as those in the Elberton data.

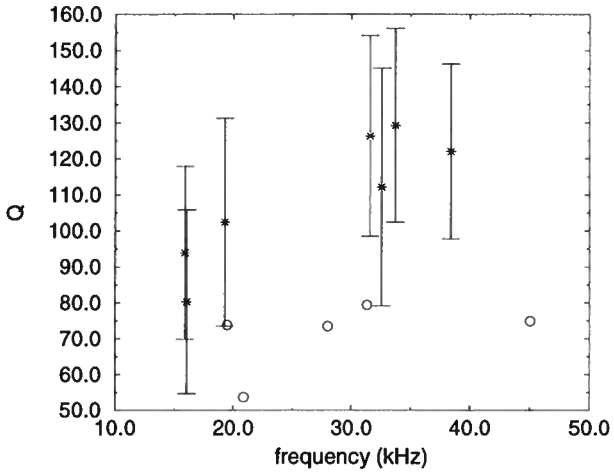

Figure 7. Modal Q as a function of frequency for both samples. Circles are data points for the Llano granite, stars for the Elberton. Error bars were not available for the Llano data set, however the Q values of the two samples are close enough to be considered within error if a similar standard deviation is assumed for the Llano as was found for the Elberton. This shows that the bulk attenuation properties of the two samples are similar, indicating that in the absence of scattering the waveforms recorded on the two samples should look quite similar.

In figure 11, a window near the beginning of the data set is shown. In the Elberton data, we can see the first arrival (P) as well as the first surface wave (R1) and the twice reflected arrival (PPP). In the Llano data it is possible to see the first arrival and the first surface wave, however the arrivals are less clear and the PPP wave is no longer visible. On both data sets there is another coherent, flat arrival between the first arrivals and the first surface wave arrivals, marked PP?. The time at which this wave arrives is consistent with both a wave travelling along the surface at the bulk medium velocity and a wave that reflects off of the surface of the sample half way between the source and receiver (see figure 8). The reason these raypaths would be unaffected by the anisotropy is that both paths have sampled the medium in a number of directions. The stacked data, figure 12, show the surface wave arrivals more clearly for both samples.

Figure 13 shows power spectra of the two data sets. Although the two spectra have similar shapes, the amplitude of the spectrum for the Llano data is lower at higher frequencies. The difference is not large however, and could be caused by the slightly lower Q of the Llano sample. The 2 MHz roll off of the spectra is largely caused by the response of the vibrometer which has a nominal maximum frequency of 1.5 MHz.

The second feature of interest is in the first arrival

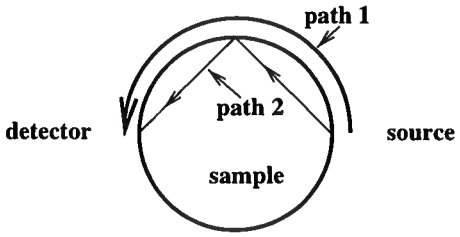

Figure 8. The two possible raypaths that explain the PP? arrival. The kinematics of the two raypaths are so close that it is impossible to differentiate between them kinematically. We are currently working on determining which path is contributing to the data set. Either path will average over a large area of the sample, thus neither path is expected to exhibit the anisotropy seen in the first arrivals.

data. The first arrival times vary significantly as a function of angle. This violates our assumption that the coherent portion of the waveform is constant around the sample and means that our particular choice of ensemble is not just an ensemble over the randomness of the medium but also over the anisotropy of the medium. This means that to extract information about the heterogeneity of the samples we must take into account the fact that not all of our 'coherent' signal is independent of angle. The first arrivals, for example, are coherent in that they occur regardless of the angle ϕ, but the exact arrival time depends on ϕ, so this portion of the coherent signal is not independent of angle.

In the Llano granite, the first arrivals are not as clear as they are in the Elberton data and the velocity function shows the sinusoidal structure less clearly. One possible reason for this is that the source characteristics may change as a function of angle; since the grain size is large compared to the width of the source pulse, our source signature is slightly different depending on what type of grain the pulse is focused on. The first arrival times were used to compute velocities which were fit with a sinusoidal function, shown in figure 14. Taking the amplitude of the sine function over the average velocity gives anisotropy of 11% for both samples. These values agree with those in (Bur *et al.*, 1969) and (Nur, 1971). The sine functions which best fit the data, in the least squares sense, are:

$$254\sin(2\phi - 3.7) - 24\sin(4\phi - 5.8) + 4434,$$

for the Elberton and

$$271\sin(2\phi - 5.0) - 116\sin(4\phi - 5.5) + 4724,$$

for the Llano.

In (Backus, 1965) and (Smith & Dahlen, 1973) the azimuthal dependence of velocity on angle, in a weakly anisotropic media, was found theoretically to be of the form:

$$v(\phi) = A + B\sin(2\phi + \psi_1) + C\sin(4\phi + \psi_2), \qquad (1)$$

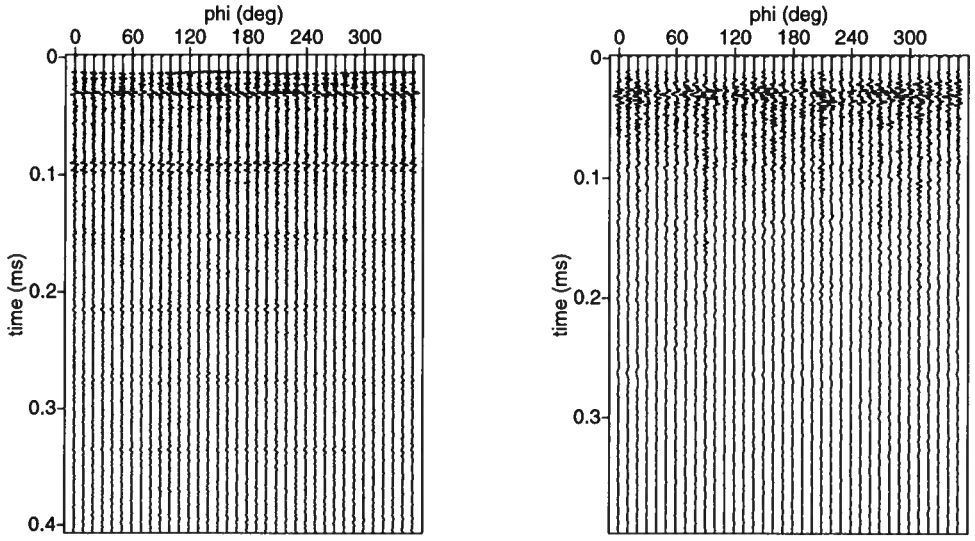

Figure 9. Raw waveforms, showing the difference in signal amplitude between the two samples. The left plot is data for the Elberton granite and the right is data for the Llano granite. The sampling rate is 10 MHz for the Elberton and 25 MHz for the Llano in all plots. The surface waves are easily visible in the Elberton data however in the Llano it is difficult to see these arrivals because of the incoherant nature of the data at late times.

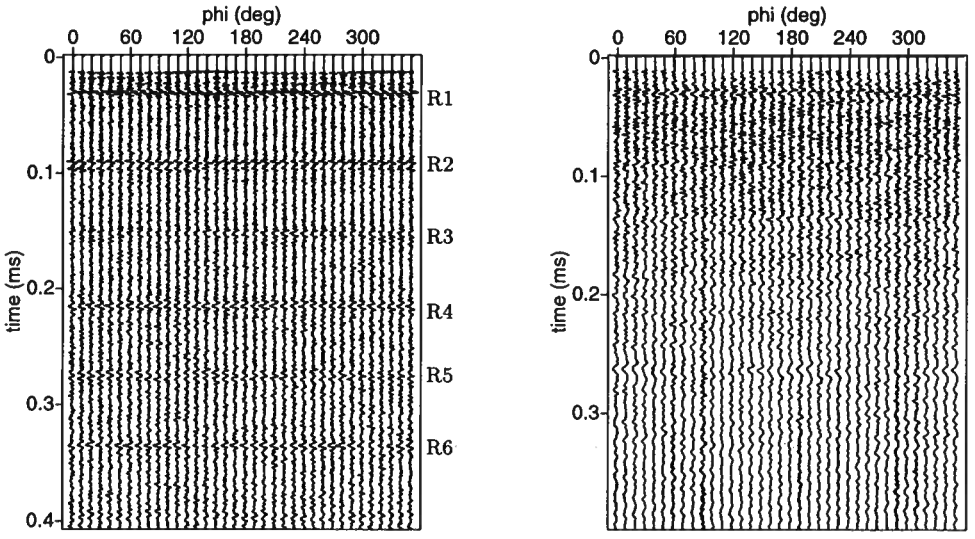

Figure 10. This data set has agc gain applied to it, to bring out the later time features. The left plot show waveforms for the Elberton granite and the right waveforms for the Llano granite. It is now possible to see the surface wave arrivals in both data sets although they are still difficult to separate from the rest of the signal on the Llano data set, due to grain scattering.

although in (Smith & Dahlen, 1973) and (Smith & Ekström, 1999) it is stated that the 4ϕ dependence does not seem necessary in fitting most data. We see that, for the Elberton sample, our results are clearly in agreement with this finding. For the Llano sample it seems at first that the 4ϕ dependence is significant. The data residuals from fitting the data with only a 2ϕ dependence are not significantly larger than when the 4ϕ dependence is included however, indicating that the anisotropy may not be the only factor controlling the variation in arrival time. The angular dependence of this anisotropy also explains why the surface waves do not show evidence of anisotropy. This is because the surface waves average the function in equation 1 over π radians and $\int_0^\pi sin(n\phi)d\phi = 0$ if n is even.

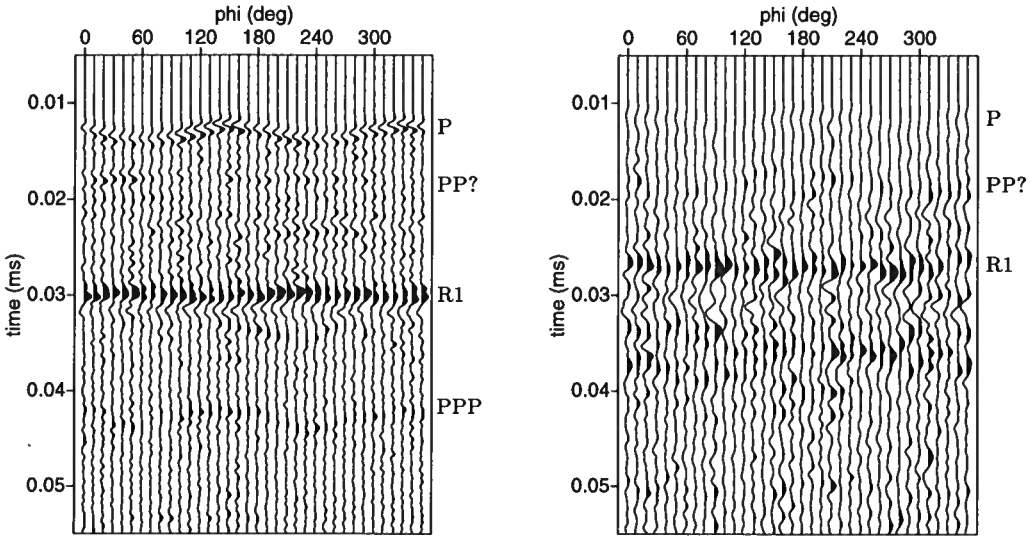

Figure 11. This figure shows an early time window in the data, in the Elberton (left) the first arrival (P), first surface wave (R1) and first reflection (PPP) are clearly visible. In the Llano data only the first arrival and surface wave are visible. The PP? arrival is kinematically explained by at least two different raypaths. Since it does not show the anisotropy in the first arrivals, it must be explained by a raypath that has travelled in different directions through the samples.

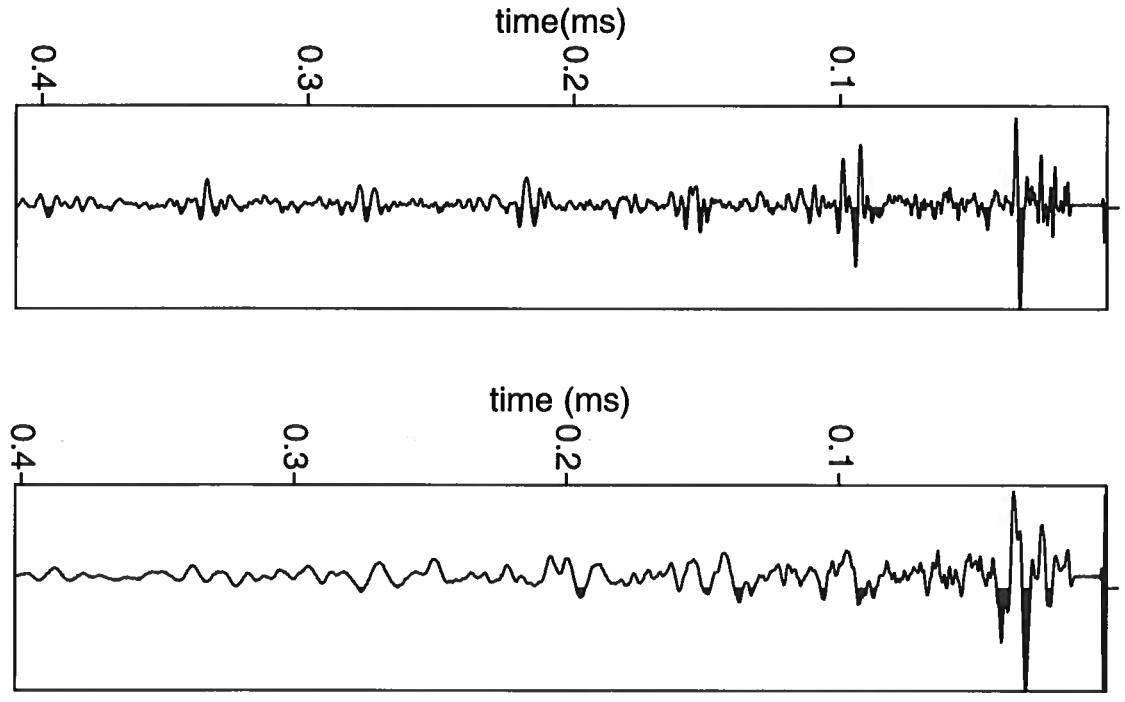

Figure 12. The stacked data show the deterministic signal, the surface waves are apparent on both data sets though to a lesser degree on the Llano (Elberton is on the top, Llano on the bottom). Much of the later time amplitude has been spread out due to scattering in the Llano sample and so this trace appears to have lower amplitude than does the Elberton. The first arrival has lower amplitude than expected in both cases due to the anisotropy of the samples.

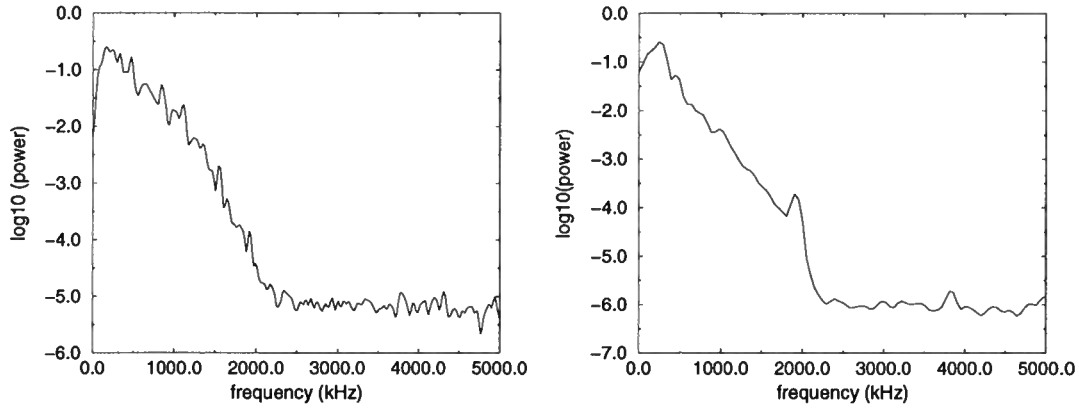

Figure 13. This figure shows the power spectrum of the data. The peak frequency is about 500 kHz. The Llano spectrum is smoother than the Elberton because the sample density is higher in the Llano data set than in the Elberton.

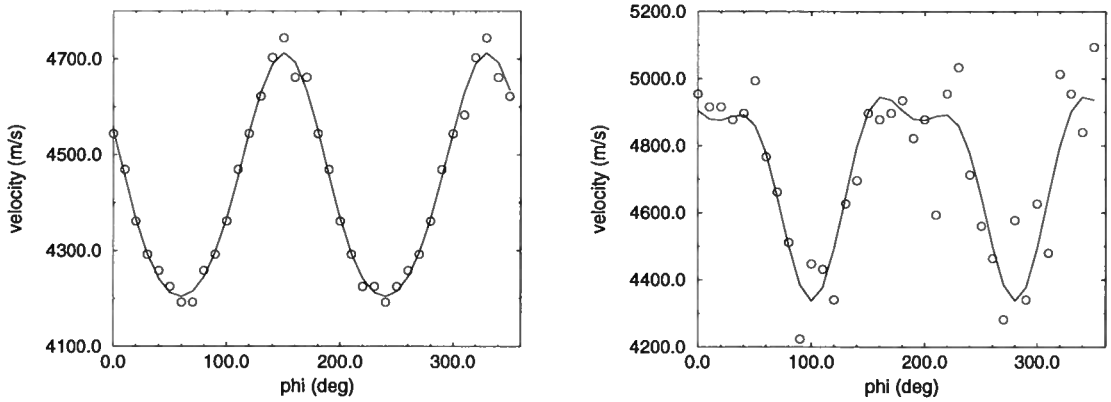

Figure 14. This figure shows the velocities, computed from the first arrivals in the data set. The Elberton data (left) show a clear sinusoidal dependence on angle while the Llano (right) show a larger degree of scatter and the sinusoid, shown as a solid line, is a poorer fit to the data in this case. The angular dependence of the velocity is in agreement with theoretical results from Earthquake seismology which predict a 2ϕ and 4ϕ dependence of velocity as a function of angle in a weakly anisotropic medium.

Discussion

We have shown preliminary measurements of ultrasonic waveforms in granular media using a non-contacting methodology. The speed of the technique allows us to quickly make rotational scans of rocks; these scans illustrate the strong fracture induced body wave anisotropy present in granite samples. This ultrasonic anisotropy is consistent with previous measurements using resonant spectroscopy. In a fine-grained sample, we see coherent waveforms at very long times, corresponding to 6 surface wave round trips. However, in a coarse grained sample, which has similar moduli and Q, the waveforms rapidly de-cohere due to grain scattering. Our ultimate goal is to be able to use the incoherent, multiply scattered waveforms to make inferences about the microstructure of rock samples. Not only would this provide new insights for rock properties characterization, but it would help lay the foundation for diffuse wave imaging and inversion methods in seismology.

Acknowledgments

This work was partially supported by the US Army Research Office under grant #DAAG55-98-1-0070, the National Science Foundation under grant #EAR-0111804 and by the sponsors of the Consortium Project on Seismic Inverse Methods for Complex Structures at the Center for Wave Phenomena. The authors would like to

thank Roel Snieder for continuing helpful discussions on the results presented here.

REFERENCES

Backus, G.E. 1965. Possible forms of seismic anisotropy of the uppermost mantle under oceans. *JGR*, **70**, 3429–3439.

Bur, T.R., Hjelmstad, K.E., & Thill, R.E. 1969. An ultrasonic method for determining the attenuation symmetry of materials. *Bureau of Mines Report of Investigations*, **7335**, 1–8.

De Rosny, J., & Roux, P. 2001. Multiple scattering in a reflecting cavity: Application to fish counting in a tank. *J. Acoust. Soc. Am.*, **109**.

Le Rousseau, J.H.L., Zadler, B., Scales, J.A., & Smith, M.L. 2002. Resonance ultrasound spectroscopy: theory and application. *preprint*.

Nur, A. 1971. Effects of stress on velocity anisotropy in rocks with cracks. *Journal of Geophysical Research*, **75**, 2022–2034.

Scales, J.A., & Van Wijk, K. 2001. A tunable multiple-scattering system. *Applied Physics Letters*, **79**.

Scruby, C.B., & Drain, L.E. 1990. *Laser Ultrasonics techniques and applications*. Bristol: Adam Hilger.

Smith, G.P., & Ekström, G. 1999. A global study of Pn anisotropy beneath continents. *JGR*, **104**, 963–980.

Smith, M.L., & Dahlen, F.A. 1973. The azimuthal dependence of Love and Rayleigh wave propagation in a slightly anisotropic medium. *JGR*, **78**, 3321–3333.

Snieder, R., Gret, A., Douma, H., & Scales, J.A. 2002. Coda wave interferometry for estimating nonlinear behavior in seismic velocity. *Science*, **295**, 2253–2255.